



PERGAMON

International Journal of Solids and Structures 39 (2002) 3429–3449

INTERNATIONAL JOURNAL OF  
**SOLIDS and**  
**STRUCTURES**

[www.elsevier.com/locate/ijsolstr](http://www.elsevier.com/locate/ijsolstr)

# Some observations of volumetric instabilities in soils

David Muir Wood

*Department of Civil Engineering, University of Bristol, Queen's Building, University Walk, Bristol BS8 1TR, UK*

Received 13 February 2002

---

## Abstract

The direct shear apparatus was developed for soil testing because it reproduced the shear failure surfaces that formed a part of the failure mechanism of many geotechnical systems. Typical shear tests on dense sands show a softening load:displacement response which is associated with significant volumetric expansion. While shear localisations can be detected from discontinuities in marker layers, the change in density can be detected using radiography. The progressive formation of shear localisations is readily observed in situations which impose a discontinuity of boundary displacement and these can naturally be interpreted as precursors to a failure mechanism. However, more subtle patterns of volumetric strain or density localisation can be observed in situations where no such obvious boundary displacement discontinuity exists but the sand body is subjected to a more general shearing. Such patterns have a structure which is clearly related to the size of the sand particles. Several examples of such patterns are presented and implications for soil testing and for model tests on soils are discussed. © 2002 Elsevier Science Ltd. All rights reserved.

**Keywords:** Sand; Shearing; Dilation; Localisation; Scale effects

---

## 1. Introduction

Classically, much of geotechnical engineering design and analysis has proceeded on the basis of ultimate limit state calculations for which estimates of strength of soils form a primary input. Latterly, as the power of readily available computing has increased, the possibility of performing serviceability limit state analyses of the performance of geotechnical systems under working loads has improved. Such analyses require as input constitutive descriptions of deformation characteristics of soils. Evidence of strength and deformation characteristics comes from laboratory tests on soil samples. While some of these tests may nominally attempt to apply controlled stresses and strains to single elements of material, observations made external to the sample reveal system response rather than material response. However, it is often tempting to assume that things that we choose not to observe do not exist and to attempt to remain blissfully unaware of the distinction between the system and the element. Absence of evidence is not the same as evidence of absence.

Validation of numerical analyses of performance of geotechnical systems—boundary value problems—is readily achieved through comparison of discrete boundary measurements (for example, the settlement of a foundation, the displacement of a wall) but comparisons with response internal to the soil mass are less

---

*E-mail address:* [d.muir-wood@bristol.ac.uk](mailto:d.muir-wood@bristol.ac.uk) (D. Muir Wood).

straightforward. Delving inside the soil in a way which does not disturb the response that is being observed is not always easy. Internal measurement of stresses always runs into problems of the relative stiffness of the soil and the stress measurement device—we will not consider stresses any further. This paper is concerned, rather, with presentation and discussion of some of the patterns of internal deformation in soil models revealed primarily using radiography and the relationship of such patterns to the formation of shear localisation and failure surfaces in soils.

There is some looseness in the terminology that is used. Radiography can detect density variations and hence the effects of localised dilation. The result may be patterns of ‘dilation bands’. These have often been interpreted as indicators of ‘localisation of shear deformation’ and hence ‘shear bands’, ‘ruptures’ or ‘failure surfaces’. However, it is suggested here that instability in volumetric response leading to clear contrasts in density, and hence patterns of dilation bands, is not *necessarily* linked with classical shear localisation. Detail of the circumstances under which bifurcation of shear or volumetric response (or both) can occur is naturally linked with the constitutive behaviour of the soil. That link is beyond the scope of the present paper which attempts to present some of the observations as challenges to the constitutive modellers. Suffice it to say that the more interesting phenomena that are being presented come from situations where rotation of principal axes of stress and strain is certainly significant. Most data against which constitutive models have been validated have come from element tests in which the principal axes are fixed. The confidence attached to modelling of response under rotating axes is much lower.

## 2. Radiographic determination of strain fields and dilation bands

Radiography has been used since at least the early 1960s (Roscoe et al., 1963) to observe the changing position of lead shot markers in, usually, plane strain soil models and elements (Fig. 1a). Lead shot absorb X-rays much more than the soil mass leaving clear images on the X-ray film. Displacements of a more or less regular grid of shot from one film to the next can be interpreted as indications of a continuum displacement field and, through differentiation, a corresponding strain field (Fig. 1b). Evidently, for such an interpretation to be appropriate, the spacing of the grid of lead markers must be large by comparison with individual particle sizes so that the assumption of continuum response can be accepted as reasonable.

While radiography provides a relatively non-invasive technique for locating the current positions of lead or other opaque markers, study of radiographs reveals other effects which come from local changes in the soils themselves. Local and relatively confined density changes, if sufficiently marked, produce corresponding contrasts in absorption of X-rays which can be seen on the radiographs (Fig. 2). Such density variations are linked with particle rearrangements and local changes in soil microstructure.

## 3. Direct shear box

Observation of slope failure in stiff overconsolidated clays shows that the mechanism of failure typically involves sliding of one block of soil on another block of soil separated by a thin failure surface. Such observations led Collin (1846) to devise the original direct shear apparatus in an attempt to measure the strength of soils when a narrow failure surface is forced to develop. The shear box in its modern form (Fig. 3a) is only marginally developed from the form used by Collin.

External monitoring of shear box tests on dense sand reveals a non-monotonic relationship between shear load and shear displacement (Fig. 4a). This shearing response is accompanied by volume changes as the sheared sand dilates (Fig. 4b). Broadly, the rate of dilation with continued shearing depends on the friction mobilised in the plane of shearing (Fig. 4c)—with the maximum rate of dilation (volumetric increase, fall in density) being approximately associated with the peak of the load:displacement relationship.

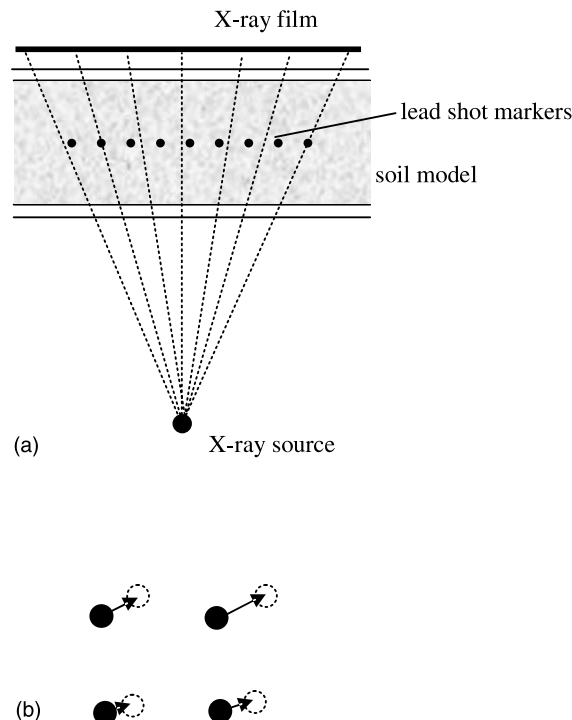


Fig. 1. (a) Radiographic technique for monitoring of soil models and (b) determination of strain field from displacements of grid of lead markers.

Generalisation of such observations of volume change can be used to generate plastic flow rules as a basic ingredient of constitutive models for sands (for example, Gajo and Muir Wood, 1999).

The external observation of shear box response, in which volume or density change is apparently linked with the forced formation of a thin shear band, makes it easy to take the observation of density variation in radiographs of soil samples as an indication of the development of a similar shear failure. Volume changes, or dilation bands, then become an observable surrogate for detection of shear localisation.

The shear box test obviously has to be interpreted as a *system* and there can be no convincing attempt to propose that the conditions within the sample being tested are in any way uniform. It is traditionally assumed that soil deformation is concentrated in a thin horizontal failure zone separating the top and bottom halves of the box in which the soil remains essentially undeformed (Fig. 3b). In fact, the internal soil behaviour is not quite as simple as this: radiographic studies show that the finite deformability of the soil trapped in the top and bottom halves allows some compression to occur in front of the leading edge and the development of an inclined dilation band at each end of the box defining a small triangular 'dead' zone (Fig. 3c). Given the forced displacement discontinuity at each end, it is not unreasonable perhaps to interpret this dilation band as a shear localisation.

#### 4. Failure surfaces/displacement discontinuities

Direct detection of the location of failure surfaces (displacement discontinuities) in the field or in laboratory model tests can be achieved by extensive post-test exhumation in clays (which is expensive and time

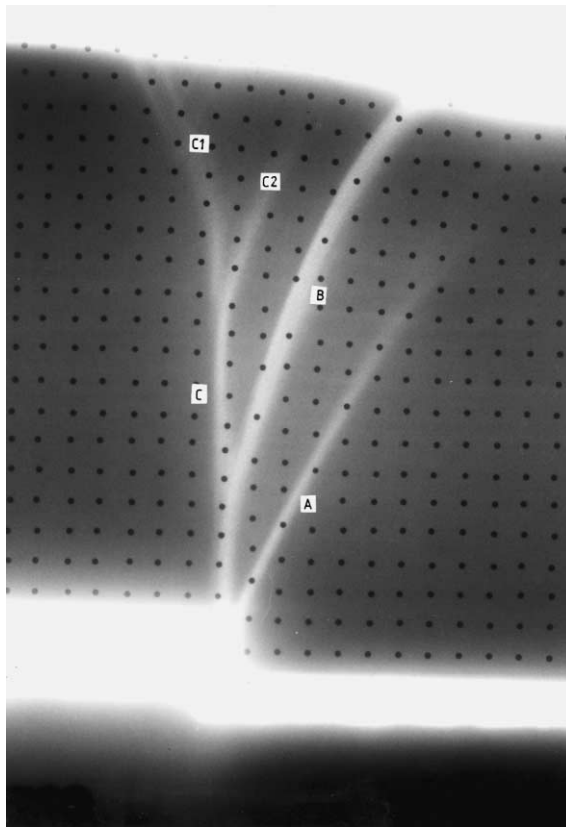


Fig. 2. Radiograph of successive dilation bands in model trapdoor test. Depth of sand bed  $\approx$  200 mm (Stone, 1988).

consuming) or from the development of discontinuities in marker layers. Kinks can be detected in failure surface detectors in the field: an equivalent in the laboratory is the use of strands of spaghetti in clay models. These take up moisture from the clay and become sufficiently flexible to move with the clay but again require exhumation. An equivalent indication of failure surface location can be found from revelation of sand columns used to model stone column foundations (Muir Wood et al., 2000). Injected columns of lead paste (or other material opaque to X-rays) can be observed non-destructively by radiography to detect discontinuities (Fig. 5) (Airey et al., 1985). All these techniques typically give discrete observations which can be linked to deduce the form of a probably continuous failure surface. They give direct indication of displacement discontinuities but are not able to provide quantitative information about the accompanying volume changes and, besides, in clay models the thickness of the displacement discontinuities is very small and the gradient of displacement locally very high. (Dudoignon et al. (2001) report the reorientation and crushing of kaolin clay particles occurring in a shear band of thickness 20–30  $\mu\text{m}$ .)

The superficial, external interpretation of the shear box suggests a simple model for the mechanical behaviour of sands along a displacement discontinuity. Taking the boundary measurements (Fig. 4) as an indication of the behaviour of a quasi-homogeneous thin region of soil, the direction of relative movement of the two sides of the thin region, and hence the rate of volume increase, is deduced to depend on the angle of dilation and hence angle of friction mobilised on the displacement discontinuity (Fig. 4c). Very roughly, the angle of dilation is of the order of the difference between the current mobilised angle of friction and the critical state angle of friction. As the relative displacement increases, the sand dilates, the available strength

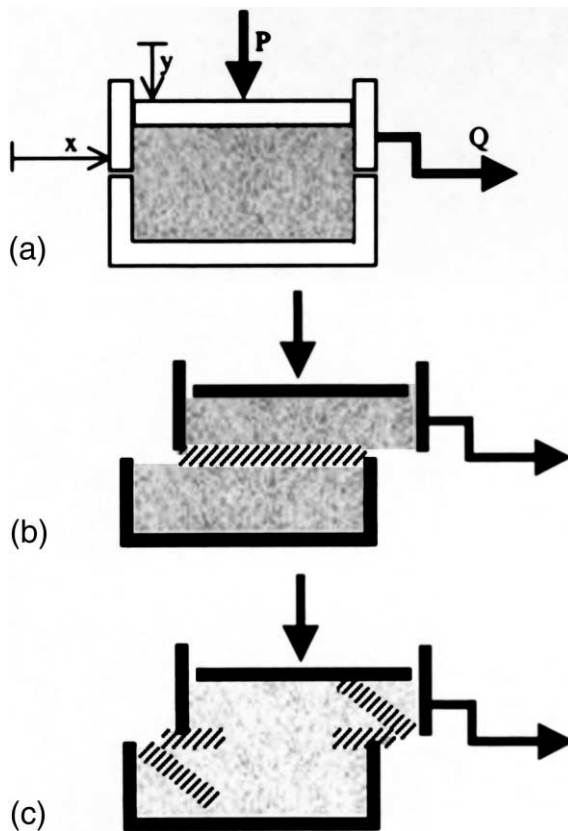


Fig. 3. (a) Schematic diagram of direct shear box; (b) idealised interpretation of shear box and (c) expected pattern of dilation bands in shear box.

falls and the rate of volume increase falls correspondingly. Eventually the sand is able to continue shearing at essentially constant volume and constant angle of friction in a so-called critical state. This model leads to a clear understanding of the pattern of the succession of dilation bands that forms in situations where there is an applied boundary discontinuity of displacement. The shear box itself provides one obvious example. Other examples are provided by the trapdoor problem and the rotating blade (Fig. 6).

A radiograph of a trapdoor model test conducted in the laboratory at single gravity is shown in Fig. 2. This can be regarded as a cumulative image showing all the dilation bands of concentrated density change that have developed during the lowering of the trapdoor. The images of the lead markers are also clearly visible but it is evident that the calculation of strains loses its validity when the marker grid is intersected by these dilation bands. The bands form in sequence as indicated. As the trapdoor is lowered the sand near the edge of the door is intensely sheared, it dilates at an angle linked with a peak angle of friction and the dilation band A propagates at an angle to the vertical equivalent to this angle of dilation—in this case about 25°. As relative shearing displacement increases, the mobilised angle of friction reduces towards the critical state, the angle of dilation of the dilated sand falls towards zero and the orientation of this initial dilation band is no longer optimal for continued downward movement of the trapdoor. Band B forms next and the combination of high dilation on this band together with some continuing movement on band A provides kinematic compatibility with the continuing trapdoor lowering. This band subsequently also becomes kinematically undesirable and band C forms. In principle, eventually, continuing lowering of the trapdoor

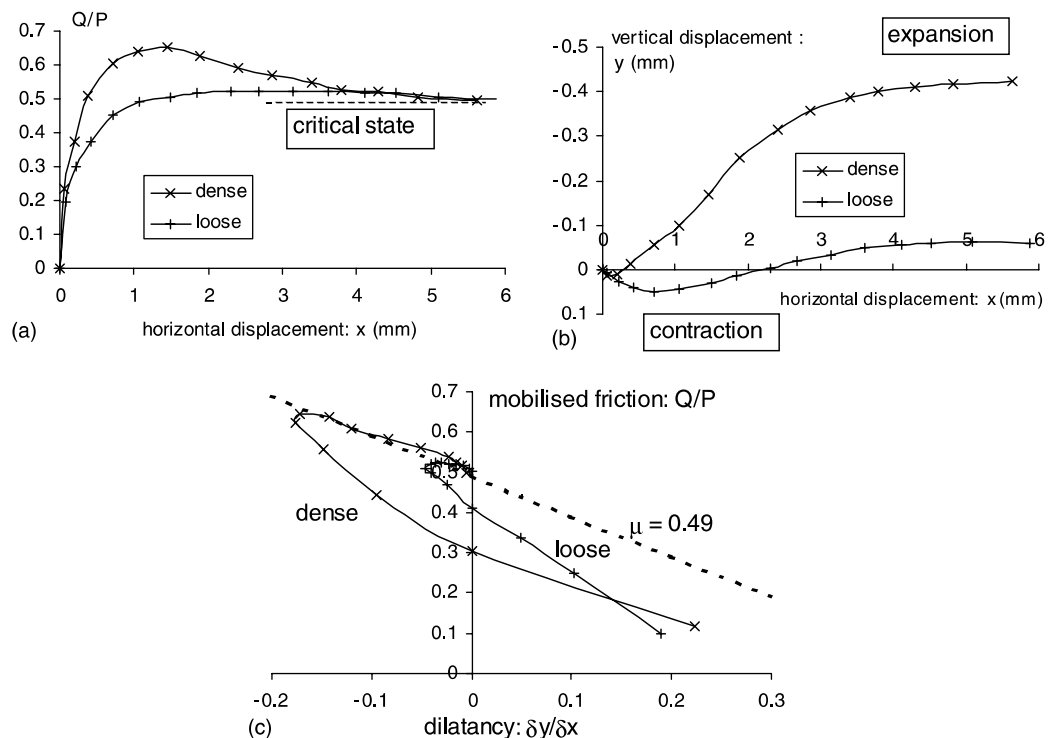


Fig. 4. Shear box tests on loose and dense Ottawa sand (data from Taylor, 1948): (a) shear force and shear displacement; (b) vertical and shear displacements and (c) link between mobilised friction and dilatancy.

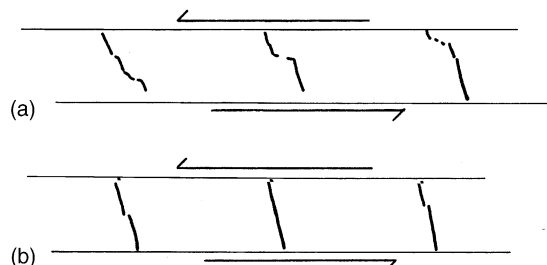


Fig. 5. Failure surfaces in simple shear test on sketched from discontinuities in threads of lead paste: (a) kaolin and (b) Gault clay (Airey et al., 1985).

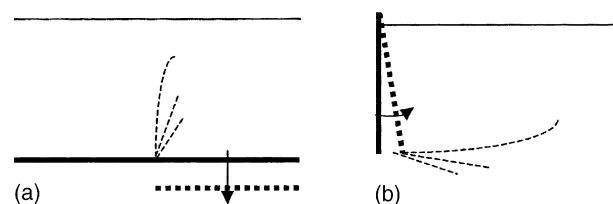


Fig. 6. Examples of geotechnical systems involving discontinuities of applied boundary displacement: (a) trapdoor and (b) rotating blade.

would be accompanied by critical state shearing on a single vertical band extending to the free surface of the sand.

The sequence of dilation band formation is shown in Fig. 7 as a function of trapdoor displacement scaled with particle size,  $d_{50}$  (the particle size for which 50% by weight of any sample is finer). The sands used are rather narrowly graded so that  $d_{50}$  gives an indication of the dominant particle size. Results are shown for three sands with  $d_{50} = 0.4$ , 0.85 and 1.5 mm. The mechanisms of deformation as revealed in the patterns of dilation bands are very similar provided the trapdoor displacement is scaled with the particle size.

A similar interpretation can be given for the sequence of dilation bands observed radiographically for the rotation of a blade into a mass of dense sand (Fig. 6b)—again with different values of  $d_{50}$  (Fig. 8). The interaction between boundary kinematic constraints and changing material dilatancy is apparent in each case. The observations do not in this case permit quite such detailed analysis of the link between the evolving mechanism of deformation and the movement of the toe of the blade scaled with the particle size. However, comparison of the 7/14 and 14/25 sands shows the larger blade movement required to produce an equivalent mechanism for the coarser sand. The finer, 25/52, sand reveals three successive dilation bands: unlike the coarser sands, the second band (B) has not reached the free surface before the changing dilatancy forces the switch to a new mechanism.

The shear box itself can now be revisited. Scarpelli (1981) described some radiographic studies that were performed on sand tested in a rather simple long shear box. The general arrangement is essentially the same as in the standard direct shear apparatus in Fig. 3a; however, the box is constructed out of wood and the length can be adjusted between 65 and 330 mm. The sample height is fixed at 26 mm and the width 51 mm. Some of these results were reported by Scarpelli and Wood (1982) using the maximum length of sample and further observations were made by Hartley (1982) using various different lengths of shear box. Initial response of the sand is like the translation of a pair of anti-symmetrical facing vertical blades into the sand, and initial dilation bands form at an angle to the horizontal at each end (Fig. 9a). With shorter boxes the

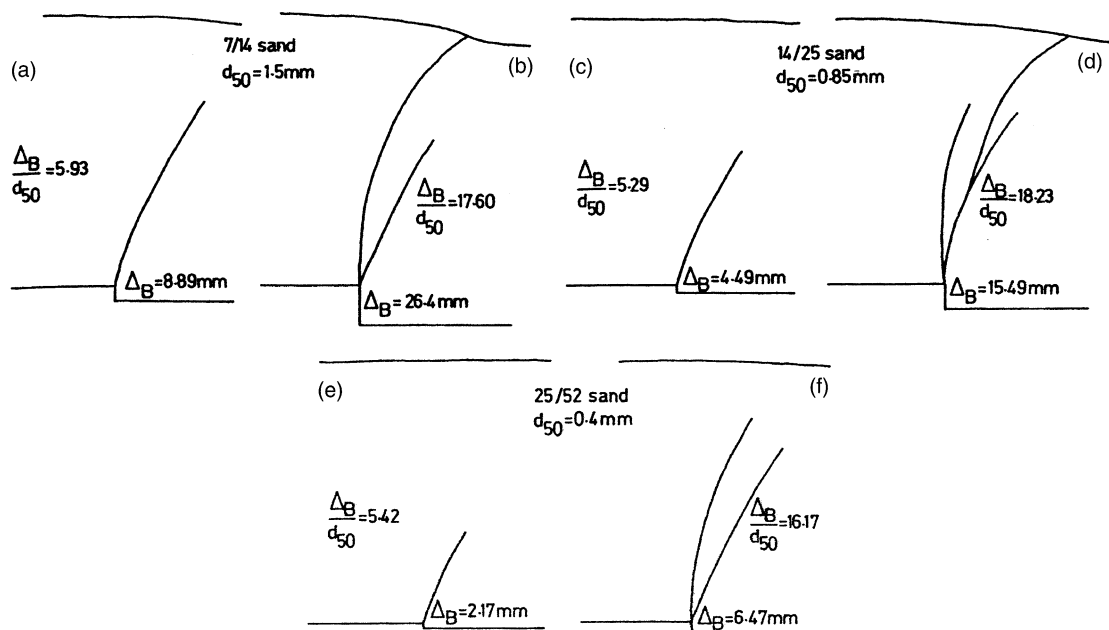


Fig. 7. Sequence of dilation band formation in model trapdoor tests: (a, b) 7/14 sand  $d_{50} = 1.5$  mm; (c, d) 14/25 sand  $d_{50} = 0.85$  mm and (e, f) 25/52 sand  $d_{50} = 0.4$  mm ( $\Delta_B$ : trapdoor displacement) (Stone and Muir Wood, 1992).

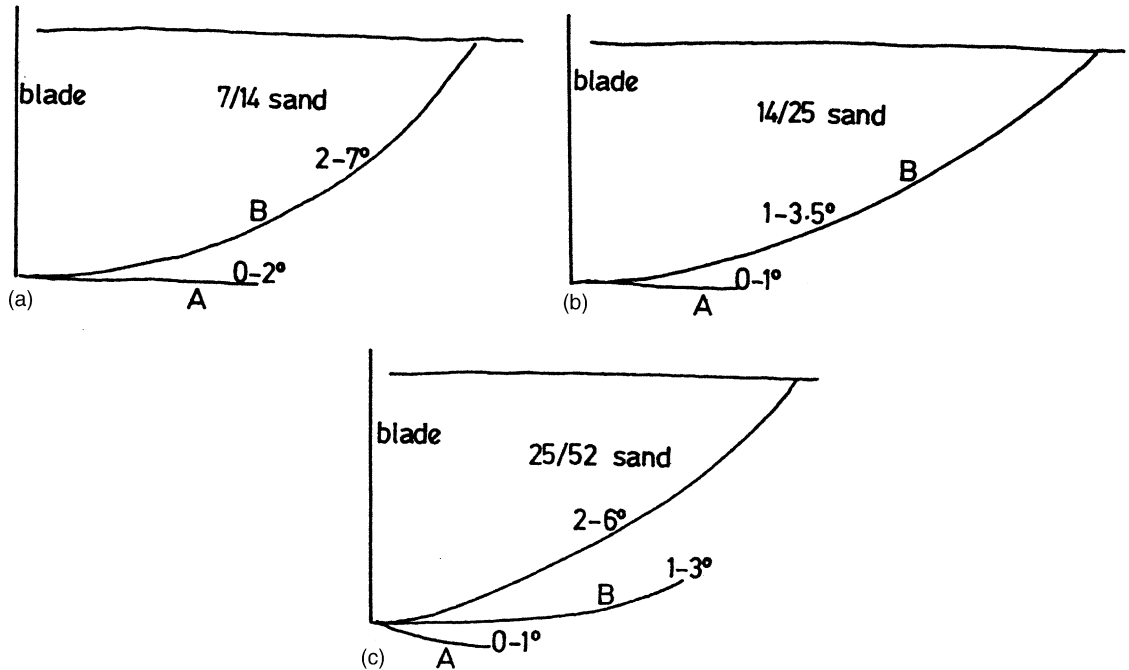


Fig. 8. Sequence of dilation band formation in front of rotating blade: (a) 7/14 sand; (b) 14/25 sand and (c) 25/52 sand (Stone and Muir Wood, 1992).

next band forms across the box, sub-horizontally (Fig. 9b)—the presence of the rigid top and bottom horizontal boundaries provides kinematic constraint absent in the rotating blade configuration. With longer shear boxes more complex patterns are observed and the fully developed band may happily form

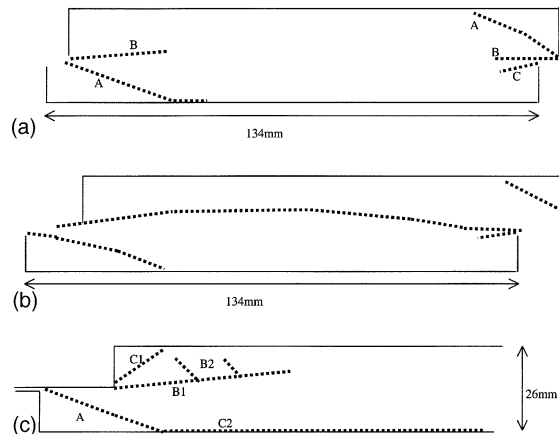


Fig. 9. (a) Initial dilation bands observed in long shear box test on dense sand (length 134 mm): sequence of formation A, B; (b) subsequent pattern of dilation bands observed in 134 mm box and (c) pattern of dilation bands observed in long shear box test on dense sand (length 330 mm: left third box shown): sequence of formation A, B1 & B2, C1 & C2. Sketches from radiographs (Scarpelli, 1981; Hartley, 1982).

along the top or bottom boundary rather than along the plane separating the two halves of the box (Fig. 9c).

## 5. Dimensions of dilation bands

The radiographic observation of density variations can also be used to estimate the thickness of shear bands and formed the basis of Roscoe's (1970) often quoted statement that "failure surfaces [deduced from dilation bands interpreted as shear bands] in our models are of the order of ten grains thick"—an assertion which has been widely accepted. However, radiographic evidence of dimensions of shear bands is rather imprecise. A band only becomes visible when the accompanying volume or density change can be discerned—the tip of a propagating band is inevitably obscure.

Theoretical support for a link between shear band thickness and grain size has been provided both from a statistical mechanics approach (Bridgwater, 1980) leading to an estimate of thickness of eight particle diameters, and from a plasticity analysis using Cosserat theory (Mühlhaus and Vardoulakis, 1987) which leads to typical estimates of thickness of sixteen particle diameters.

Oda and Kazama (1998) describe the transmission of load, through columns of particles across shear bands, inspired by photoelastic observations of plane assemblies of elliptical particles. They deduce that the maximum number of particles that can be involved in a buckling column is about 10 and found shear band thicknesses of 7 to 8 times mean particle size from microscopic studies of thin sections of sand samples.

Constitutive models such as the hypoplastic Cosserat continuum model used by Tejchman (1994) introduce particle size as an input parameter in order to give the model some necessary characteristic length. Since such models are still continuum models the behaviour of individual particles is not of concern but a dimension of shear band thickness emerges as an output. Tejchman deduces a thickness of about 15 particle diameters based on the presence of significant Cosserat rotations. Knowledge of shear band thickness thus becomes a valuable parameter for calibration of appropriate constitutive models.

Extensive radiographic measurements made by Scarpelli (1981) and Hartley (1982) in the long shear box suggest that the ratio of dilation band thickness to average particle size varies along the band. The observed dilation bands appear to be typically thinner at their tips, where they are propagating into the sand, and reach a steady value only where dilation has finished and the sand is shearing at a critical state (Scarpelli and Wood, 1982). The theoretical work of Mühlhaus and Vardoulakis (1987), however, seems to imply an expectation that a shear band will decrease in thickness with continuing deformation.

A shear/dilation band can only exist within a soil mass (in a granular material it has to have a finite thickness involving a finite number of soil particles) and its direction of development is controlled by the conditions of dilatancy that obtained at the moment of its formation. However, as deformation continues on the band, the dilatancy conditions will change, the current direction of the band may no longer be kinematically optimal, and some of the apparent thickening of shear/dilation bands that has been observed may result from attempts by the soil in the region of the band to involve some of the surrounding soil in the deformation process in order to relax the kinematic constraints. The apparent dilation band thickening is then locked into the radiographic records of density variation even if the active thickness at any stage is much less. The experiments described by Vardoulakis (1978) show the progressive reduction in mobilised friction and mobilised dilatancy towards critical state values in a simple biaxial test specimen requiring relative movements across the band of the order of 2 mm representing a corresponding shear strain of about 40% in dense Karlsruhe sand. The treatment by Drescher and Michalowski (1984) of a shear band as a shock through which material may pass with accompanying density change recognises that a shear band is not necessarily fixed with reference to the material.

Precise definition of the boundaries of a dilation band on a radiograph is somewhat subjective. Because of the nature of granular material it is not possible for there to be a sharp edge to the band. The radiograph

Table 1  
Radiographic observations of shear band thickness

Test type	Sand grading	Particle size $d_{50}$ (mm)	Rupture thickness $t_z$ (mm)	$t_z/d_{50}$	Reference
Long shear box	100/170	0.12	1.7	14.2	Hartley (1982)
	30/52	0.40	3.8	9.5	
	14/25	0.90	9.0	10.0	
Long shear box	30/52	0.40	Up to 5.5	Up to 13.75	Scarpelli (1981)
Rotating blade	25/52	0.4	4–5	10–12.5	Stone (1985)
	14/25	0.85	9–15	10.5–17.6	
	7/14	1.5	11–20	7.3–13.3	
Biaxial test	Fine	0.2	3.7	18.5	Mühlhaus and Vardoulakis (1987)
	Medium	0.33	4.3	13	

provides an average indication of X-ray absorption over the full width of the soil mass; whether or not this provides a true projection of the band thickness depends on the relative positions of the X-ray head and the dilation band. The band may not actually develop orthogonally to the sides of the soil mass. Stone (1985) shows the curved surface exposure of the fully developed shear bands in sand models where side friction impedes soil movement. Oda and Kazama (1998) note that the shear band thicknesses that they deduced from radiography generally slightly overestimated the thicknesses deduced from inspection of micro-structure.

A number of quoted values of radiographically determined dilation band thicknesses are listed in Table 1. These have been obtained under three different experimental situations: in a long shear box (Scarpelli, 1981; Hartley, 1982), in front of a blade rotating about its top (Stone, 1985), and emerging from a density inhomogeneity in a biaxial test (Mühlhaus and Vardoulakis, 1987).

Stone's figures deliberately show a range because of the subjectivity involved in assessing dilation band thickness. The smaller values indicate the thickness of the lightest region of the radiograph, indicating lowest absorption of X-rays. The larger values indicate the width of the region within which density variation is certainly occurring—the grayness of the radiograph is clearly different from that for the undilated sand.

## 6. Experimental observation of displacement gradient

Though the dilation band is observed in a radiograph as a region of high volume change, this volume change is assumed to be associated with the localisation of shear strain within this thin region. Localisation of shear strain implies a high gradient of shear strain, and hence high displacement gradient. Displacements in granular soils have generally been determined radiographically only at discrete markers—where lead shot have been placed within the soil—and determination of detailed local profiles of displacement is not possible. With coarse grained soils, however, conventional photography can be used to follow the movements of individual soil particles, observed through a glass side plate of the model. Measurement from such photographs can reveal rather local displacement profiles. However, there is some evidence that with such coarse materials side friction breaks the plane strain symmetry to a lesser extent than with finer grained materials and, besides, the photography is not giving an average response but the response on a particular section where the particles are moving against the glass boundary.

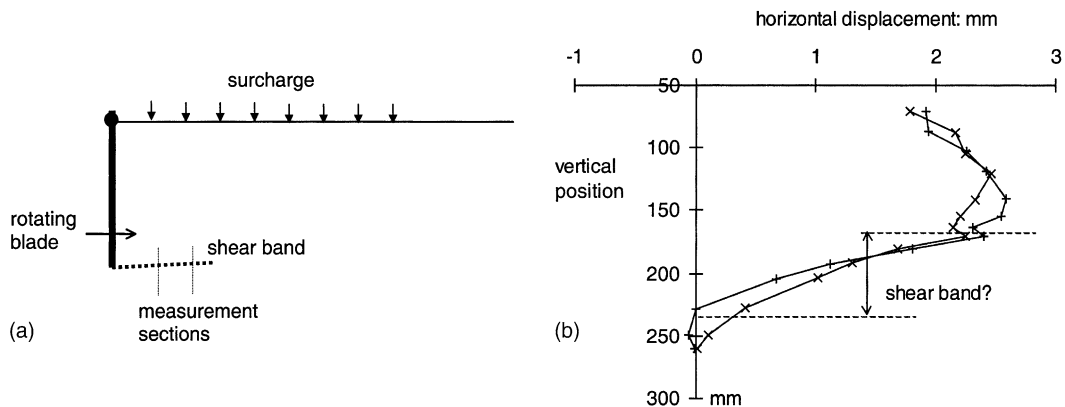


Fig. 10. (a) Measurement of particle displacements in front of rotating blade and (b) profile of horizontal displacements for blade rotation  $3^\circ$  to  $3.5^\circ$ ,  $d_{50} = 3$  mm, surcharge 70 kPa.

As part of a continuing study of dilation/shear band formation in soils, a series of tests has been performed in which a blade 275 mm high by 167 mm wide was rotated about its top into a bed of granular material with or without a surface surcharge being applied (Fig. 10a). The results of radiographic observation of tests on finer materials have already been quoted in Table 1. However, the tests included tests using a fine sub-angular gravel, with 90% lying between the 3/16" and No. 7 sieves (between about 5 and 2.5 mm,  $d_{50} = 3$  mm) for which radiographic observation was less helpful. Results are quoted from a test in which a surcharge of 70 kPa was applied at the surface of the soil (although radiographic observations showed no consistent pattern of influence of stress level on shear band thickness).

For total blade rotations of approximately  $3^\circ$  and  $3.5^\circ$ , relative displacements of individual particles were measured on two vertical profiles roughly 50 and 90 mm in front of the blade. The blade displacement of  $0.5^\circ$  represents a displacement of 2.4 mm at the toe of the blade. The measured displacement profiles are shown in Fig. 10b. The origin on the vertical axis is arbitrary; the horizontal axis shows the measured displacements in a direction parallel to the shear band which runs across the profiles.

Fig. 10b shows that the soil particles are moving together roughly as a rotating 'rigid' block above the putative shear band (which is sub-horizontal (Stone and Muir Wood, 1992)) and are stationary below it. The transition occurs over a distance of about 60 mm though some particle adjustments are occurring a further 10–20 mm each side. This transition distance of 60 mm implies a shear band thickness of about 20 particle diameters. The upper edge of the shear band, interpreted now as the region of highest displacement gradient, appears to be rather more sharply defined than the lower edge. The observations reported by Stone and Muir Wood (1992) demonstrate clearly that as deformation progresses and dilatancy reduces, the orientation of the active shear band rotates anti-clockwise towards the blade. The top of the observed shear band is thus entering into virgin material whereas the bottom is moving out of material which has previously been sheared. For the coarse material, this transition occurs rather slowly.

Previously shear band thicknesses have been determined from observations, usually using radiography, or dilatancy which is the consequence of the shearing of a dense granular material. The present observations are linking shear band thickness to displacement gradient: it may be more important to characterise and reproduce this aspect of the constitutive behaviour in numerical calculation of soil response in boundary value problems. Neither observation is exclusive; however, the displacement gradient is measured over an increment of deformation and does therefore indicate the region of the granular material which is presently participating in the shearing, whereas observations of dilatancy tend to be cumulative and can only with difficulty distinguish changes in dilation band thickness that have occurred during any one increment of

boundary displacement and are therefore much more sensitive to the changes in kinematic control of band orientation which will lead to shifts of the location of an active dilation/shear band relative to the particles which originally contributed to its formation.

Direct measurements of particle movements (and rotations, which the present study has not reliably measured) have been used to establish shear band dimensions in numerical simulations of shearing of two-dimensional assemblies of circular particles by Bardet and Proubet (1991) among others. They conclude that the shear band width in a simulated biaxial compression test decreases with axial strain from 18 to 15 times the average particle diameter (their assembly had two sizes of particle). Such studies, and the present observations, suggest that the zone within which particles are certainly aware of and influenced by the intense shearing in the shear band may be wider than would be deduced from measurements of dilatancy alone.

## 7. Dilation bands in presence of imposed shearing

Where there is a clear source of boundary discontinuity, such as the edge of a footing, trapdoor or wall, the analogy with the shear box seems clear and the use of the zone of volumetric dilation as an indicator of the localisation of shear deformation and formation of an evolving failure surface is reasonable. However, there are other configurations of boundary displacement which do not impose displacement discontinuities but nevertheless lead to clearly visible regions of density change in radiographs. Three examples will be given, which may be seen as related to the trapdoor, blade and shear box described previously.

Tests have been performed (Stone, 1988) in which part of the support of a layer of soil is rotated away from the soil as shown in Fig. 11a. In each test, the soil layer was about 200 mm thick. The base of the soil container was covered with a thin sheet of latex which was roughened with sand so that it can be assumed that the base of the soil is subjected to essentially vertical movement with a discontinuity of slope but not of displacement. Tests have been performed both at single gravity and on a geotechnical centrifuge (Schofield, 1980) at an equivalent acceleration of 100 gravities. Geotechnical centrifuge modelling allows the generation of prototype stress levels in small models so that effects of stress level can be eliminated in model tests. Thus, in a test performed at 100 gravities the stresses are augmented 100-fold and at the base of a model 200 mm deep the stresses correspond to those in a prototype at a depth of 20 m. All the tests reported here were performed on dry sand prepared by pluviation to give repeatable uniform densities.

Single gravity models have been monitored using radiography. Radiography is not possible with a model 'in flight' on the centrifuge but photographic monitoring of the plane section of the model through a glass sided container is feasible. It is not possible easily to detect density variations but step movements in marker layers can be revealed to provide indication of development of failure surfaces.

Sketches from radiographs of the single gravity models are shown in Fig. 12 for three different rather single sized gradings of sand. These sketches show the dilation bands that are revealed from density contrasts in the radiographs. It is clear that there are two different phenomena occurring. At low base rotations, a pattern of sub-parallel somewhat curved dilation bands develops. These bands have a spacing that is evidently controlled by the particle size: the separation is rather greater than the thickness of the bands—perhaps of the order of twice the band thickness. It does not seem that there is significant shear displacement on each of these bands but rather that they represent a spontaneous switch of the density of the sand from homogeneous to regularly heterogeneous. For the two coarser materials (14/25 sand,  $d_{50} = 0.85$  mm, 7/14 sand,  $d_{50} = 1.5$  mm), the pattern clearly contains two intersecting complementary sets of bands. As base movement increases further, typically just one of the dilation bands (marked E in Fig. 12) develops into a shear band which extends towards the free surface of the sand. Evidently the dilated sand has lower density and therefore less available strength (Been and Jefferies, 1985; Gajo and Muir Wood, 1999)

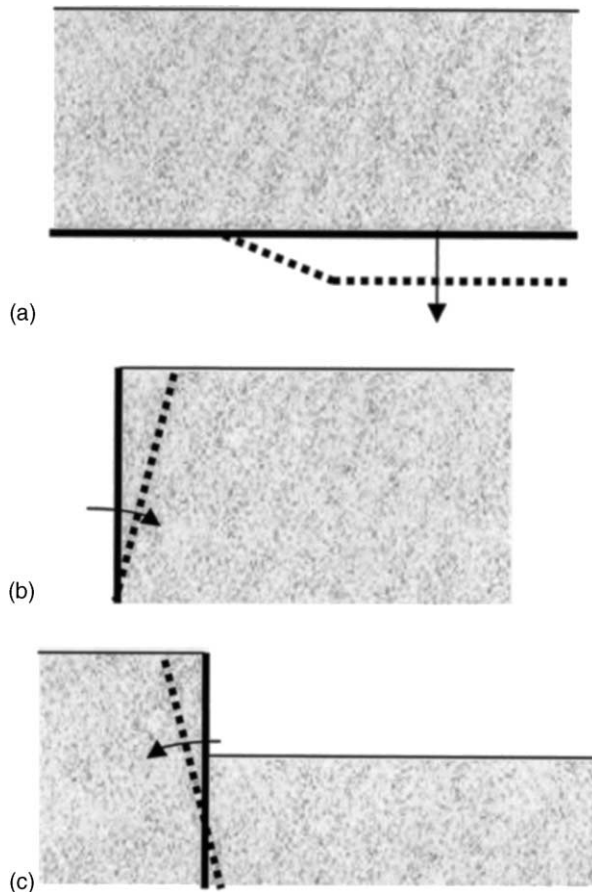


Fig. 11. Examples of geotechnical systems involving boundary rotations: (a) rotating basal support for soil layer; (b) blade rotating about toe and (c) blade rotating about intermediate height.

than the sand in the intervening undiluted material so it is not surprising that an eventual shear localisation should develop within the weaker material.

It is not possible to observe such volumetric heterogeneity in the centrifuge models. Sketches of the marker bands at a late stage of the test are shown in Fig. 13. The response is similar in character for each of the three sands but the detail is different. In each case, a shear discontinuity is seen to occur at point A as a mode II shear fracture in the middle of the sand layer well away from the boundaries. This discontinuity extends up and down from A and is joined by further discontinuities developing from B and then C. One might draw a link between the discontinuity A in Fig. 13 and the developed dilation band E eventually seen in the radiographs of the single gravity tests (Fig. 12).

A second set of tests has been performed in which a rough wall of height 330 mm was rotated about its toe into a bed of dense Leighton Buzzard sand with  $d_{50} = 0.85$  mm (Fig. 11b) (James and Bransby, 1970). Again this is a situation where the profile of imposed boundary displacements has a discontinuity of slope but not of value. The contrast of the radiographs (used primarily for monitoring the changing position of lead markers) is not high but sketches of dilation bands at different stages of wall rotation have been made and are shown in Fig. 14. Similar conclusions can be drawn. There is a dominant set of bands extending away from the rotating wall. There is evidence of an intersecting set of complementary bands. As wall

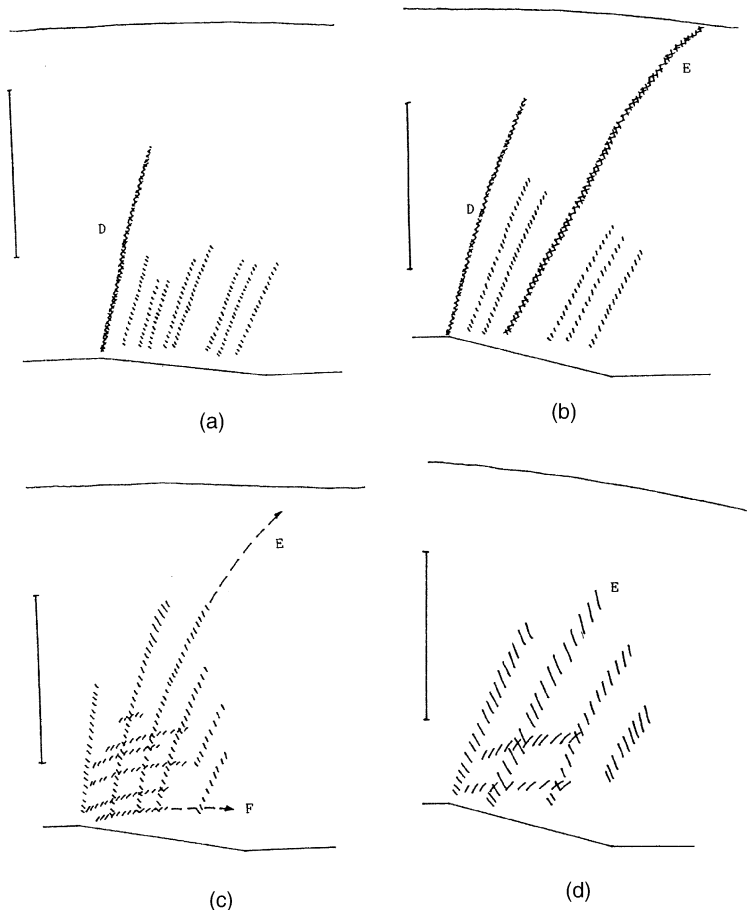


Fig. 12. Dilation bands seen in rotating basal support tests: (a) 25/52 sand, rotation 8.3°; (b) 25/52 sand, rotation 13.7°; (c) 14/25 sand, rotation 10.9° and (d) 7/14 sand, rotation 15.1°. Sketches from radiographs; vertical bar = 100 mm (Muir Wood and Stone, 1994).

rotation continues one or two of the first set of bands develop into shear bands which extend out to the free surface of the sand to create a 'fault escarpment'.

A print of a radiograph for a wall which is rotated about a point at roughly mid-height is shown in Fig. 15 (Archive of Radiographs, Cambridge University Engineering Department). The top of the wall is pushing into the sand on its left and generating a set of dilation bands similar to that shown in Fig. 14. One or two of these develop into shear bands extending to the surface. The wall is also moving away from the sand to its right and here a very clear pattern of two intersecting sets of bands is apparent in the region that is deforming in Rankine 'active' mode.

Where complementary sets of dilation bands are visible the angle of intersection in each of the examples shown in Figs. 12, 14 and 15 is typically around 65°. We are here seeing what might be termed 'spontaneous regular volumetric heterogenisation' occurring at a very low stress level. In a single gravity test, the vertical stress at a typical depth of about 100 mm is only 2 kPa. Very few reliable data are available for the stress:strain and strength behaviour of sands at such low stress levels. Stroud (1971) describes simple shear tests conducted on the 14/25 Leighton Buzzard sand with normal stress levels down to 1 psi (7 kPa) and

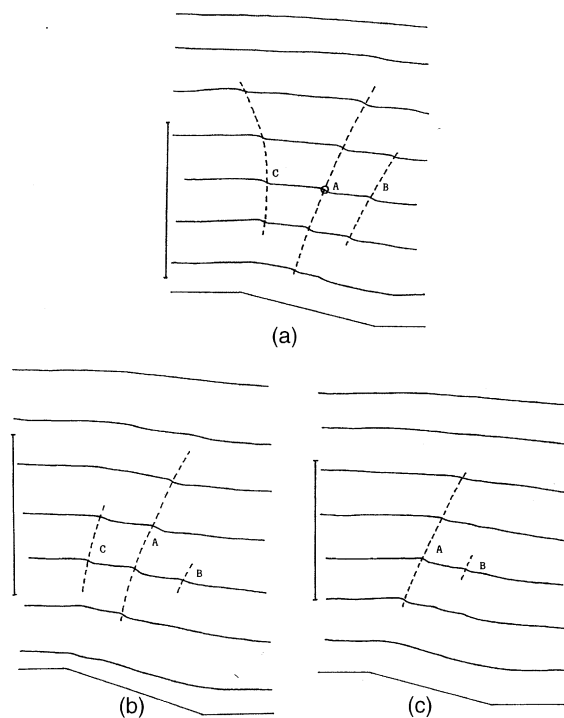


Fig. 13. Discontinuities in marker layers in centrifuge model (100g) rotating basal support tests: sequence of formation A, B, C: (a) 25/52 sand; (b) 14/25 sand and (c) 7/14 sand. Vertical bar = 100 mm (Muir Wood and Stone, 1994).

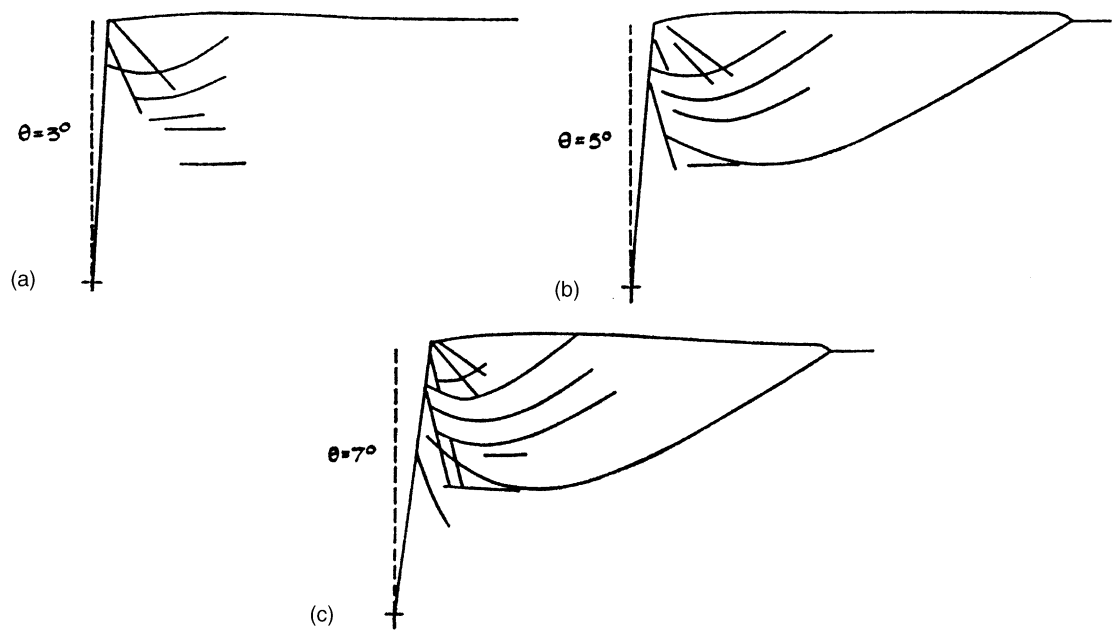


Fig. 14. Dilation bands seen in front of blade rotating about toe into 14/25 sand: (a) rotation 3°; (b) rotation 5° and (c) rotation 7°. Sketches from radiographs (James and Bransby, 1970).

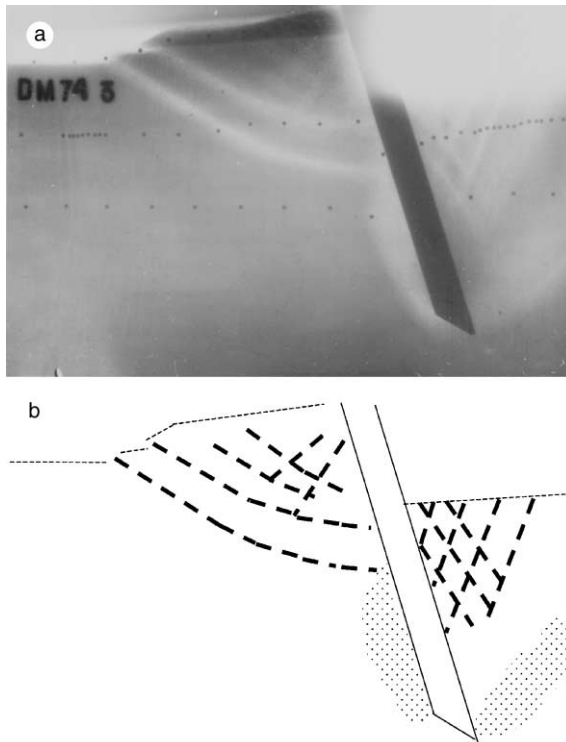


Fig. 15. Radiograph of dilation bands around model wall rotating around point at roughly mid-height (Archive of Radiographs, Cambridge University Engineering Department).

shows that at the lowest stress level the peak mobilised friction may be as high as  $\phi \approx 55^\circ$  with corresponding angle of dilation of  $\psi \approx 25^\circ$ .

The detail of the stress state inside a soil mass can never be reliably known; radiographic pursuit of the movement of lead markers can give an indication of the nature of the assumed continuous strain and strain increment state. Roscoe (1970) and others have regularly averred that the dilation bands that were seen in radiographs (called by him 'rupture surfaces') are aligned with directions of zero extension within the soil and therefore that the angle of intersection of these bands should be the 'Roscoe' angle  $\theta_R = (\pi/2 - \psi)$ . If the orientation of the bands is somehow linked with the attainment of limiting frictional stress states, then the angle of intersection should be the 'Coulomb' angle  $\theta_C = (\pi/2 - \phi)$ . Working from a simple incremental elastic-plastic model, Vardoulakis (1980, 1988) has shown that various bifurcation orientations are possible but that in the absence of imposed kinematic constraints the angle of intersection should take the 'Vardoulakis' value  $\theta_V \approx (\pi/2 - \phi/2 - \psi/2)$ . Arthur et al. (1977) present experimental data from various laboratory apparatus which seem to support the notion that the intersection angles between dilation bands (which they call 'rupture layers') should take one of these three values depending on the nature of the constraints that are imposed. The observed angles of intersection reported here seem to lie nearer the Roscoe angle,  $\theta_R$ , than either of the other possibilities. Though this may be coincidental, it corresponds with the expectation that this spontaneous heterogenisation will be strongly kinematically constrained.

It is not possible to discern the orientation of directions of principal stresses in these model tests. In analysis of radiographic observations of dilation bands in active conditions behind a flexible wall, Leśniewska and Mróz (2000) assume that the outward directed bands are aligned at  $(\pi/4 - \phi/2)$  with the vertical but in the patterns that they present the intersection angle is again nearer a Roscoe angle,  $\theta_R$ .

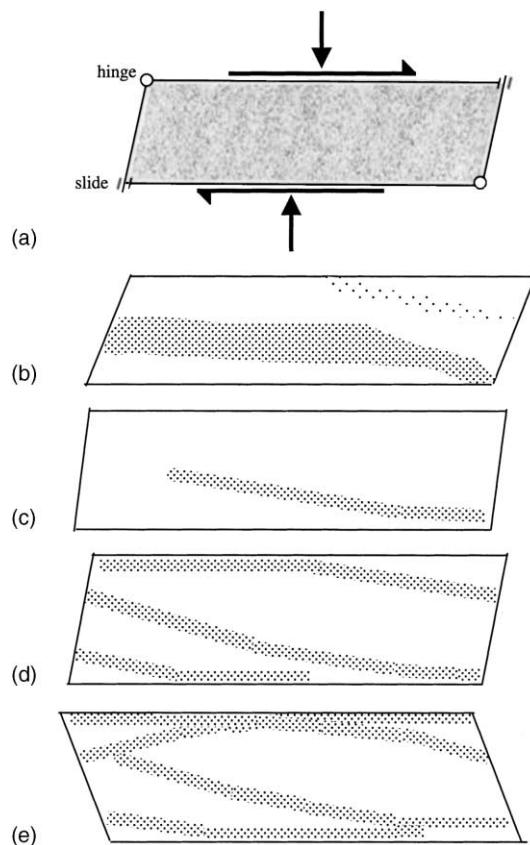


Fig. 16. (a) Schematic diagram of simple shear apparatus; initial sample height 20 mm; (b) sketch of dilation band in radiograph of simple shear test on 14/25 sand (Stroud, 1971) and (c, d, e) sketches of dilation bands in radiograph of simple shear test on fine Delft sand: (c) 7% forward shearing; (d) 15% forward shearing; (e) 32% reverse shearing (Budhu, 1979).

A third example of the formation of dilation bands in the presence of imposed shearing is provided by radiographs of simple shear tests on a fine sand (Fig. 16). The dimensions of the Cambridge simple shear apparatus (Fig. 16a) (Stroud, 1971; Budhu, 1979) were eventually chosen with a particular sand—14/25 Leighton Buzzard sand—in mind. This rather single sized sand has a mean particle size  $d_{50} = 0.85$  mm. The initial height of the simple shear sample—20 mm—was chosen so that it would neatly contain a single dilation band of canonical thickness ( $20 \times d_{50} = 17$  mm). A sketch of a radiograph of a simple shear test on this sand is shown in Fig. 16b. Although the dilation band does not occupy the whole height of the sample, it is clearly sub-horizontal in orientation so that the mechanical response observed at the boundaries of the sample is primarily controlled by the behaviour within the band. It may be noted that the simple shear apparatus imposes an overall strain constraint of zero extension in the horizontal direction. (There is some indication of a subsidiary inclined dilation zone at the top right of the sample.)

However, with a finer Delft sand,  $d_{50} \approx 0.2$  mm, but with the same initial height of sample, the kinematic constraint is much less. An inclined dilation band is observed (Fig. 16c) at a shear strain of about 7%—well before the peak in the mobilised friction on the boundary of the sample. By 15% shear strain this has been joined by two other bands (Fig. 16d)—each following a similar inclination but merging into the rough top and bottom faces of the apparatus to form boundary interface bands. With reversal of shearing these

dilation bands are locked into the sample and others are generated (Fig. 16e). The boundaries of the simple shear apparatus are rigid but the necessary smoothness of the ends of the apparatus results in a complex internal stress state which is certainly not expected to be uniform. There is no evidence in these radiographs of the two regular intersecting sets of dilation bands seen in the rotating wall and rotating base models.

## 8. Scale effects and laboratory modelling

Desrues et al. (1996) performed an elegant series of tests using computed radiographic tomography to detect dilation bands in triaxial test specimens. The beautiful patterns that they have observed suggest not only that volumetric heterogeneity through formation of dilation bands is the rule rather than the exception but also that internal heterogeneity does not necessarily result in major discontinuities, shear bands, that can be detected with the naked eye at the surface of the sample—for example, through an enclosing rubber membrane. However, as seen in the observations reported here, dilation bands may eventually develop into major expressions of shear localisation, as also seen in the true triaxial observations reported by Desrues et al. (1985). Desrues et al. (1996) conclude that more or less complex localisation patterns can develop in laboratory specimens, depending on test conditions, but that symmetry of the specimen state (for example, overall axial symmetry) is a stabilising factor with respect to localisation. “The stabilisation is relative: it does not suppress localisation but leads to smoother global response characteristics, and complex localisation patterns involving multiple mechanisms.” The boundary value problems shown here have no imposed symmetries, and have gradients of stresses and rotations of principal axes all of which may be expected to encourage the occurrence of localisation, seen here through the formation of patterns of dilation bands.

The goal of laboratory element testing is to gather response data from which constitutive models can be developed and with which constitutive hypotheses can be tested. These constitutive models are required for calculation of performance of geotechnical systems. The goal of laboratory model tests is to discover mechanisms of response which are relevant to the behaviour of corresponding geotechnical prototypes. There is always a danger of losing sight of the eventual application in the process of gathering data. The scale of typical geotechnical prototypes will be typically metres if not tens or hundreds of metres. Typical laboratory model soils are unlikely to have particle sizes greater than a few millimetres—soils used as construction materials may contain particles up to a few centimetres. The scale of the application is certainly large by comparison with the size of the particles. Typical laboratory models may have a scale of tens of centimetres: model dimensions are likely to be large by comparison with particle sizes but not necessarily large by comparison with some of the other intrinsic lengths that have been observed.

Laboratory testing and subsequent constitutive modelling have to come to terms with the particle-continuum duality of soils: they are particulate materials but the scale of applications is such that continuum treatment through representative volume elements is essential. Several potential scale effects have emerged from the observations reported here.

(1) Dilation bands have a thickness which, it seems to be generally agreed, is of the order of 10–20 times the typical particle size, for which  $d_{50}$  is used here as a formal indication. Most of the tests from which this generalised thickness has been deduced have been on rather narrowly graded sands—the controlling particle size will be less obvious in a more widely graded material, such as a natural glacial deposit. Unless particle sizes are large, this thickness will usually be small by comparison with typical dimensions of laboratory element tests or of laboratory models.

(2) There is a mobilisation or development length associated with the end of a shear band over which rates of dilation fall from their peak to the zero critical state value. This is harder to pin down because available data are sparse. The location of the tip of the band is only visible when enough density change has occurred to provide sufficient contrast on the radiograph. Deduction of the subsequent kinematic response

requires lead markers conveniently disposed across the band whose position is not known in advance. The difference between the mechanisms seen for fine sand and coarse sand in Fig. 8c and a, can be ascribed to the shorter end length for the dilation or shear band in the finer sand. Clearly there will be an end effect of some magnitude. Scarpelli and Wood (1982) suggest an order of magnitude of  $100 d_{50}$  in long shear box tests. Stone and Muir Wood (1992) suggest a length of about  $176 d_{50}$  from rotating blade experiments. Vardoulakis et al. (1981) produce numbers for a trapdoor experiment from which a length of about  $120 d_{50}$  might be deduced. These are now dimensions which are likely to be of the same order as typical dimensions of laboratory models. If the phenomenon being observed is primarily dependent on failure along a localised shear band, then scaling from a small model to a prototype may be erroneous.

(3) Patterns of spontaneous regular volumetric heterogenisation have been observed which have a cell size apparently typically at least about three times the thickness of individual dilation bands. This patterning emerges as a result of effects at the particle level. However, it is in no way fatal for system stability, and any simulation or calculation of response will need to continue to describe the behaviour of the patterned material. Standing back, a representative volume element containing a reasonable number of patterned cells could be regarded as an alternative pseudo-homogeneous continuum. If at least 10 cells need to be included, then a typical length of the order of  $300 d_{50}$  emerges. This sort of dimension has evident implications for selection of dimensions of laboratory tests especially where rotation of principal axes is to be controlled and studied. A simple shear apparatus with height 20 mm and length 100 mm would be restricted to soil with  $d_{50} < 0.033$  mm which represents a coarse silt. Any measurement of boundary stresses in an element test or laboratory model would also need either to average stresses over a distance significantly larger than the pattern cell or to measure at many points over a contact length which is small by comparison with this cell.

All the observations reported here have related to deformations occurring within soil bodies. As noted, internal measurement of stresses is not feasible. However, numerical analyses have been performed of two (and three) dimensional particulate assemblies in which the nature of the conversion of apparent stresses to interparticle forces can be studied. The results of Radjai et al. (1997) are typical and show that for two-dimensional assemblies of circular particles the stress is carried through force chains which form themselves into cells with typical sizes of, say, 10 particles. A similar result is seen in the photoelastic studies of force chains in two-dimensional assemblies of discs reported by Drescher and De Josselin de Jong (1972). The way in which these observations should be extrapolated to three dimensions and to realistic particle shapes is not certain but this can be taken as further evidence of ways in which length scales larger than the single particle may influence observations of response of granular materials.

## 9. Conclusion

Two types of volumetric instability have been revealed from radiographic studies of sand models. Single well-defined dilation bands have been linked with localisation of shear deformation and the progressive development of failure surfaces. Such bands define mechanisms of response in which somewhat undeforming blocks of sand slide on the failure surface. Kinematic changes may lead to switches between one mechanism and another mechanism requiring the formation of new dilation/shear bands. Such mechanisms develop especially, but not exclusively, in geotechnical systems which impose boundary displacement discontinuities which *have* to propagate into the sand. These dilation/shear bands are showing effects which can be understood at the macroscopic level—the mechanisms revealed align directly with the analytical techniques used in classical geotechnical analysis, and the dimensions of moving blocks are large by comparison both with the thickness of individual bands and with the dimensions of typical particles. Scale effects can be expected in such situations because of the ‘development length’ of the bands from the point of propagation to the point where the critical state condition is attained.

In other situations, a spontaneous regular volumetric heterogenisation seems to occur with development of patterns of dilation bands not linked to imposition of boundary discontinuities and not obviously describable as shear bands except insofar as relative movement on such bands can be accommodated by minor rearrangements at the particle level. The pattern can appear homogeneous if studied from a distance sufficiently large that representative volume elements can reasonably enclose a number of cells of the pattern. However, the conditions under which such heterogenisation occurs need further study so that its implications for the estimation of mechanisms and patterns of response of prototype geotechnical systems can be properly evaluated and the consequences for the selection of data for calibration of constitutive models assessed.

## References

Airey, D.W., Budhu, M., Wood, D., 1985. Some aspects of the behaviour of soils in simple shear. In: Banerjee, P.K., Butterfield, R. (Eds.), *Developments in Soil Mechanics and Foundation Engineering—2*. Elsevier Applied Science Publishers, pp. 185–213. Chapter 6.

Arthur, J.R.F., Dunstan, T., Al-Ani, Q.A.J.L., Assadi, A., 1977. Plastic deformation and failure in granular media. *Géotechnique* 27 (1), 53–74.

Bardet, J.-P., Proubet, J., 1991. A numerical investigation of the structure of persistent shear bands in granular media. *Géotechnique* 41 (4), 599–613.

Been, K., Jefferies, M.G., 1985. A state parameter for sands. *Géotechnique* 35 (2), 95–112.

Bridgwater, J., 1980. On the width of failure zones. *Géotechnique* 30 (4), 533–536.

Budhu, M., 1979. Simple shear deformation of sands. PhD thesis, University of Cambridge.

Collin, A., 1846. *Recherches expérimentaux sur les glissements spontanés des terrains argileux*. Carilian-Gourley et Dalmont, Paris.

Desrues, J., Lanier, J., Stutz, P., 1985. Localisation of the deformation in tests on sand sample. *Engineering Fracture Mechanics* 21 (4), 909–921.

Desrues, J., Chambon, R., Mokni, M., Mazerolle, F., 1996. Void ratio evolution inside shear bands in triaxial sand specimens studied by computed tomography. *Géotechnique* 46 (3), 529–546.

Drescher, A., De Josselin de Jong, G., 1972. Photoelastic verification of a mechanical model for the flow of a granular material. *Journal of Mechanics and Physics of Solids* 20, 337–351.

Drescher, A., Michalowski, R.L., 1984. Density variation in pseudo-steady plastic flow of granular media. *Géotechnique* 34 (1), 1–10.

Dudoignon, P., Pantet, A., Carrara, L., Velde, B., 2001. Macro–micro measurement of particle arrangement in sheared kaolinitic matrices. *Géotechnique* 51 (6), 493–499.

Gago, A., Muir Wood, D., 1999. Severn-Trent sand: a kinematic hardening constitutive model for sands: the  $q$ – $p$  formulation. *Géotechnique* 49 (5), 595–614.

Hartley, S., 1982. Shear bands in sand. Part II, Project report. Department of Engineering, University of Cambridge.

James, R.G., Bransby, P.L., 1970. Experimental and theoretical investigations of a passive earth pressure problem. *Géotechnique* 20 (1), 17–37.

Leśniewska, D., Mróz, Z., 2000. Limit equilibrium approach to study the evolution of shear band systems in soils. *Géotechnique* 50 (5), 521–536.

Mühlhaus, H.-B., Vardoulakis, I., 1987. The thickness of shear bands in granular materials. *Géotechnique* 37 (3), 271–283.

Muir Wood, D., Stone, K.J.L., 1994. Some observations of zones of localisation in model tests on dry sand. In: Chambon, R., Desrues, J., Vardoulakis, I. (Eds.), *Localisation and Bifurcation Theory for Soils and Rocks*. A.A. Balkema, Rotterdam, pp. 155–164.

Muir Wood, D., Hu, W., Nash, D.F.T., 2000. Group effects in stone column foundations: model tests. *Géotechnique* 50 (6), 689–698.

Oda, M., Kazama, H., 1998. Microstructure of shear bands and its relation to the mechanisms of dilatancy and failure of dense granular soils. *Géotechnique* 48 (4), 465–481.

Radjai, F., Wolf, D.E., Jean, M., Roux, S., Moreau, J.J., 1997. Force networks in dense granular media. In: Behringer, R.P., Jenkins, J.T. (Eds.), *Powders & Grains 97*. Balkema, Rotterdam, pp. 211–214.

Roscoe, K.H., 1970. The influence of strains in soil mechanics (10th Rankine Lecture). *Géotechnique* 20 (2), 129–170.

Roscoe, K.H., Arthur, J.R.F., James, R.G., 1963. The determination of strains in soils by an X-ray method. *Civil Engineering and Public Works Review* 58 (684), 873–876, and 58 (685), 1009–1012.

Scarpelli, G., 1981. Shear bands in sand. MPhil thesis, University of Cambridge.

Scarpelli, G., Wood, D., 1982. Experimental observations of shear band patterns in direct shear tests. In: Vermeer, P.A., Luger, H.J. (Eds.), *Deformation and Failure of Granular Materials*, Proc. IUTAM Symp., Delft. Balkema, Rotterdam, pp. 473–484.

Schofield, A.N., 1980. Cambridge Geotechnical Centrifuge operations: 20th Rankine Lecture. *Géotechnique* 30 (3), 227–268.

Stone, K.J.L., 1985. Shear band formation in granular materials. MPhil thesis, University of Cambridge.

Stone, K.J.L., 1988. Modelling of rupture development in soils. PhD thesis, University of Cambridge.

Stone, K.J.L., Muir Wood, D., 1992. Effects of dilatancy and particle size observed in model tests on sand. *Soils and Foundations* 32 (4), 43–57.

Stroud, M.A., 1971. The behaviour of sand at low stress levels in the simple shear apparatus. PhD thesis, University of Cambridge.

Taylor, D.W., 1948. Fundamentals of Soil Mechanics. John Wiley, New York.

Tejchman, J., 1994. Numerical study on localised deformation in a Cosserat continuum. In: Chambon, R., Desrues, J., Vardoulakis, I. (Eds.), *Localisation and Bifurcation Theory for Soils and Rocks*. Balkema, Rotterdam, pp. 257–274.

Vardoulakis, I., 1978. Equilibrium bifurcation of granular earth bodies. *Advances in analysis of geotechnical instabilities*. University of Waterloo Press, SM study 13, paper 3, pp. 65–119.

Vardoulakis, I., 1980. Shear band inclination and shear modulus of sand in biaxial tests. *International Journal for Numerical and Analytical Methods in Geomechanics* 4, 103–119.

Vardoulakis, I., 1988. Theoretical and experimental bounds for shear-band bifurcation strain in biaxial tests on dry sand. *Res Mechanica* 23, 239–259.

Vardoulakis, I., Graf, B., Gudehus, G., 1981. Trap-door problem with dry sand: a statical approach based upon model test kinematics. *International Journal for Numerical and Analytical Methods in Geomechanics* 5, 57–78.